IDEA StatiCa Member

WP2: Braces with Single-sided Gusset Plates Connections

Project Partner:

IDEA StatiCa

Report

Report Author

Dr. ANDREAS MÜLLER M.Sc.

MORENA GIULIERI M.Sc.

Responsible Investigator

Prof. Dr. techn. ANDREAS TARAS

Chair of Steel and Composite Structures

Institute of Structural Engineering (IBK)

ETH Zurich

Institut für Baustatik und Konstruktion
Professur für Stahlbau und Verbundbau

ETH zürich

Table of contents

1. Background Information

1.1. Introduction

In infrastructure and industrial constructions, gusset plates are often used to design and create connections for trusses or bracing systems. Slotted gusset plates are welded to hollow or I-shaped sections. These elements can then quickly be mounted and assembled with bolted connections and splice plates or simply welded to the rest of the structure. Recent construction examples, such as the gateway in Figure 1 located at the Bern railway station, illustrate the relevance of gusset plates.

In recent application cases, unusually long gusset plates were used, leading to a reduced bearing capacity. If not properly designed, such construction details may suffer from stability issues with sometimes tragic consequences. Two widely reported examples are the collapse of a scaffolding at Neurath Power Station in Germany and the catastrophic failure of the I-35W Mississippi River Bridge in the USA. Both lead to the loss of human life and serious financial consequences.

Figure 1: a) Gateway at Bern railway station; b) typical gusset plate connection [1]; c) Collapsed scaffolding from Neurath Power Station [2]; d) Collapse of the I-35W Mississippi River bridge [3]

1.2. Design problems

One of the main difficulties in practice is that the governing collapse mechanism is often a combined stability failure of the gusset plate and the steel member. Therefore, methods that design the connections and the column separately are not suitable since interactions between both elements are neglected. To overcome this shortfall, various engineering models were developed to specifically design columns with gusset plate connections, but they are not widely applied [3]. Numerical tools can be used instead, as they offer a powerful solution within the design procedure. Nevertheless, the complexity of such modeling approaches, often using shell finite element solutions, is error-prone and dependent on the problem knowledge leading to different design consequences.

The Component-Based Finite Element Method (CBFEM) has become more widespread and popular in recent years in practice and is used in the software framework of IDEA StatiCa, allowing the performance of complex nonlinear finite element simulations while accounting for the member together with its actual connections as a whole. With regard to columns and gusset plates, the implementation of realistic imperfections in the numerical model is particularly important. Therefore, the choice of eigenmodes with gusset plate connections, usually taken from linear buckling analysis (LBA), is even more important than for isolated members only and must be verified and assessed more precisely. The decisive eigenmode (imperfection shape), which ideally leads to the lowest load-bearing capacity in a GMNIA (geometrically and materially nonlinear analysis with imperfections), is not necessarily the first eigenmode with the lowest critical elastic buckling load detected by the LBA. The failure mode needs to be assessed on the basis of symmetric and asymmetric stability behavior. An exemplary representation is shown in Figure 2. It is shown throughout this report that the need to consider both eigenmodes is crucial since the difference between the load-bearing capacities when using 1st or the 2nd eigenshape (see Figure 2) might vary strongly and lead to an underestimation when using only one eigenshape.

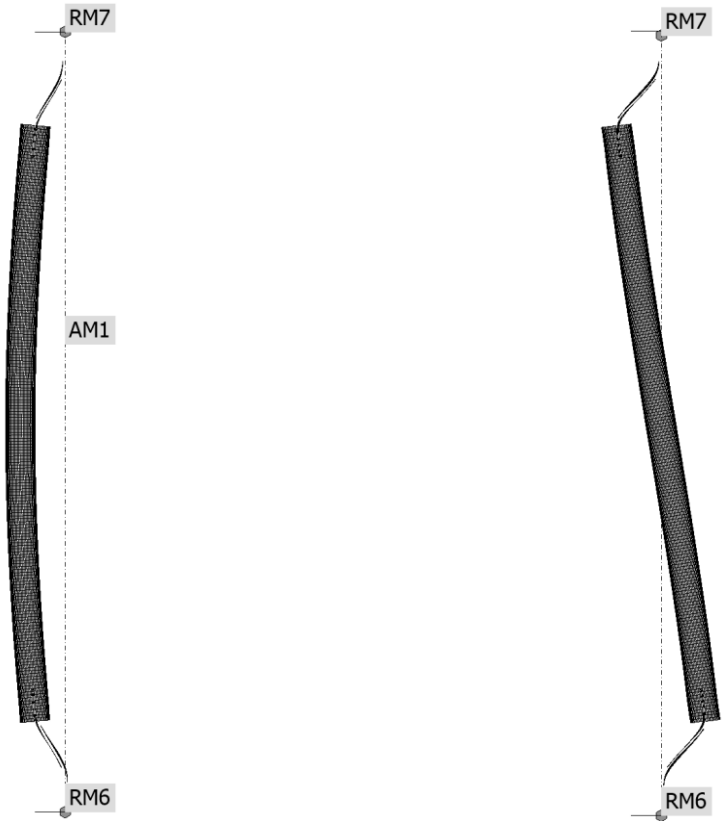

a) b)

Figure 2: LBA simulation results a) 1st eigenshape; b) 2nd eigenshape

1.3. Scope

The objective of this report is the verification of GMNIA calculations (geometrical and material nonlinear analysis with imperfections) against experimental and numerical investigations collected from the literature. The problem of using appropriate imperfection shapes and amplitudes in gusset plate connections is investigated by comparing and combining imperfection forms from LBA (linear buckling analysis) simulations. For the imperfection amplitudes, different code provisions are used, such as FprEN 1993-1-14 [4] for member imperfections and FprEN 1993-1-14 [4] and EN ISO 13920 [5] for gusset plate imperfections. The goal of this report is to specify a modeling procedure for CBFEM to safely design a compressed brace with eccentric gusset plate connections.

2. Model assumption

2.1. Background on local and global imperfection

The evaluation process proposed in this report distinguishes between **local gusset plate imperfections** and **global member/column imperfections**; see Figure 2. Local (equivalent) gusset plate imperfections, i.e., amplitudes or inclinations, are selected according to EN 1993-1-5 [7] or FprEN1993-1-14:2024 [4]; see Table 1 below (stiffener or flange subjected to twist). Those are considered to be the maximum applied limit values. The minimum gusset plate imperfection/inclination on the other hand, as the lower applied boundary, has to be chosen according to specified tolerances. EN ISO 13920 [5], which gives information on tolerances for welded constructions, was used throughout this report. Note that in all other cases, associated code provisions must be considered.

Table 1: Equivalent geometric imperfections for plate structures according to EN 1993-1-5 [6] or FprEN1993-1-14:2024 [4]

Component / type of imperfection	Shape	Magnitude
Longitudinal stiffener with length *a*	Bow	$\min(a/400, b/400)$
Panel or sub-panel with short span *a* or *b*	Buckling shape	$\min(a/200, b/200)$
Stiffener or flange subject to twist	Bow twist	$1/50$
Outstand elements for cold-formed structures – local	Buckling shape	$b/125$
Outstand elements for cold-formed structures – distortional	Buckling shape	$0{,}3 \cdot t \cdot \sqrt{f_{yb}/\sigma_{cr,d}}$

Further, global equivalent geometric imperfections are assumed for members. In general, two approaches are used, considering either a tabulated length-proportional value or a slenderness-based formulation based on the elastic critical buckling load from analytical or numerical analysis. In the following, the slenderness-dependent approach is not taken into account since the calculated eigenvalues need to be derived from members only and not, as proposed in this study, for a system containing member and gusset plates. Currently, equivalent imperfections can be chosen according to two formulations from either FprEN1993-1-1:2020 [7] or FprEN1993-1-14:2024 [4]. The formulation from FprEN1993-1-1:2020 is shown in the following and is a novel development introduced within the new code generation, taking into account the influence of external bending moments in its derivation. Background information can be taken from [8] and [9].

$$j = \frac{e_{0,d}}{L} = \frac{\alpha \cdot \beta}{\varepsilon} \tag{1}$$

where:

α	is the imperfection factor dependent on the flexural buckling curve
ε	is the material parameter considering the steel grade
β	is the reference bow imperfection
L	is the member length

Further, the modified length affine formulation is implemented in the current version of FprEN1993-1-14: 2024 [4]:

$$e_{0,d} = \frac{\alpha \cdot L}{150} \geq \frac{L}{1000} \tag{2}$$

It is based on the basic formulation from Equation (1) with the difference that the required equivalent bow imperfection is no longer a function of ε. The influence of material yielding was captured directly in the analysis during the derivation of this expression [10]. The factor β from Equation (1) was additionally calibrated to a constant value of 1/150 from 646 beam FE simulations. Note that the use of this imperfection formulation requires a modified Young´s modulus of E = 200000 N/mm^2. For detailed information on the derivation of Equation (2) the reader is referred to the work of Walport [10]. A comparison between the different formulations was done on a global member level in [11], leading to differences in the maximum reached resistance. The modified imperfection amplitude formulation from FprEN 1993-1-14:2024 tends to lead to results that are rather optimistic compared to the European buckling curves for flexural buckling, although Young´s modulus was modified (E = 200000 N/mm^2) throughout the simulations.

2.2. Modelling

In order to model properly a member connected to gusset-plates with the CBFEM program IDEA StatiCa with the software package Member, attention should be paid to some key factors. The reproduction of boundary conditions implemented in other FEM software, such as ABAQUS, or during experimental tests is of key importance. A wide library of welds, bolts, plates, and steel sections can be assembled to model a structure, but some specific idealized boundary conditions, such as a perfectly frictionless hinge, cannot be directly implemented.

To overcome this shortcoming, different solutions can be used. The gusset plate can be connected to a related member free to rotate as shown in Figure 3 a), this results in an axis of rotation slightly higher. Otherwise, the related member can be assembled to the gusset plate with a one-sided fillet weld as depicted in Figure 3 b), the program then generates equivalent

elements and multi-point constraints on one side of the plate that act similarly to a hinge. A slightly increased force may greatly reduce the bearing capacity of the structure.

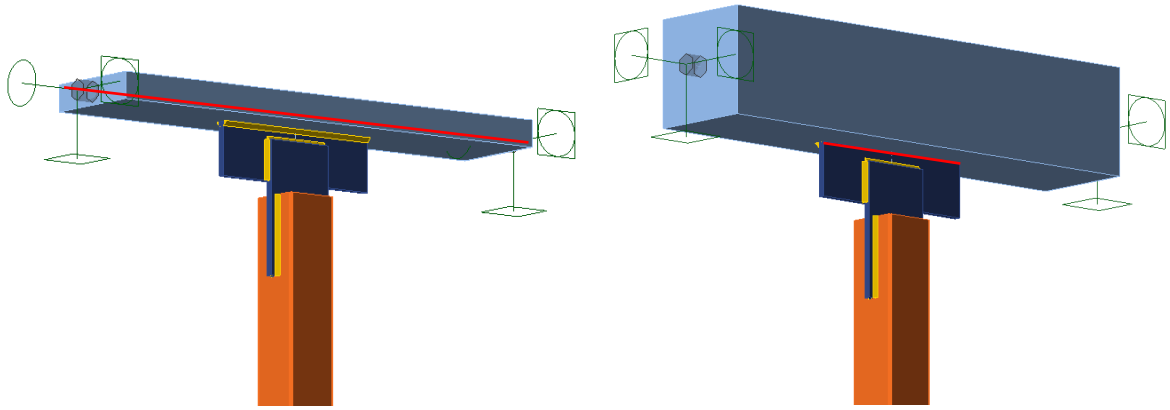

a) b)

Figure 3: Locations of the hinges (in red): a) standard hinge above the plate; b) hinge modelled as a weld

Notably, a weld that is too thin can lead to numerical instability of the FE-model. A too-small weld could lead to conservative results; therefore, the influence of this parameter should be carefully verified. An example of such a phenomena is shown in Figure 4, where the only difference between models (a) and (b) is the thickness of the weld at the support circled in red. The difference in the resistance is remarkable, with a decrease of around 13% for the thinner weld.

Weld thickness: a = 10 mm
Resistance: 687.2 kN
a)

Weld thickness: a = 5 mm
Resistance: 594.4 kN
b)

Figure 4: Comparison between models with weld thickens of 10 mm a) and 5 mm b)

The material model used in IDEA StatiCa is a bi-linear elastic-plastic. The material behaviour is based on the von Mises yield criterion; an elastic behaviour is assumed before the design yield strength, f_{yd}, is reached. Afterward, the yielding plateau has a slope of $\tan^{-1}(E/1000)$ according

to EN1993-1-5 [6]. The ultimate limit state criterion for regions not susceptible to stability failure is defined when reaching a limiting value of the principal membrane strain. The default setting is a maximum strain of 5%, as recommended in Appendix C8 EN1993-1-5 [6]. As a first attempt, the strain limit should be disabled; if the computation results in a too-high and unrealistic strain value, a maximum value should be implemented accordingly.

Once the test specimen is modelled in IDEA StatiCa an FE-analysis is performed in three steps. At first, a Material Non-linear Analysis (MNA) is carried out, followed by a Linear Buckling Analysis (LBA) where the desired eigenmodes (based on settings) are computed. Finally, the ultimate load is calculated with a Geometrical and Material Non-linear Analysis with Imperfection (GMNIA). The eigenmodes from the LBA are scaled by the choice of an equivalent geometric imperfection and used as initial imperfection shapes, which can be combined. Note that the value of the imperfection can be implemented with a positive or negative sign; this has an influence on the results, and both values should be analysed. An example of the difference in results between the negative and positive imperfections implementation is shown in Figure 5.

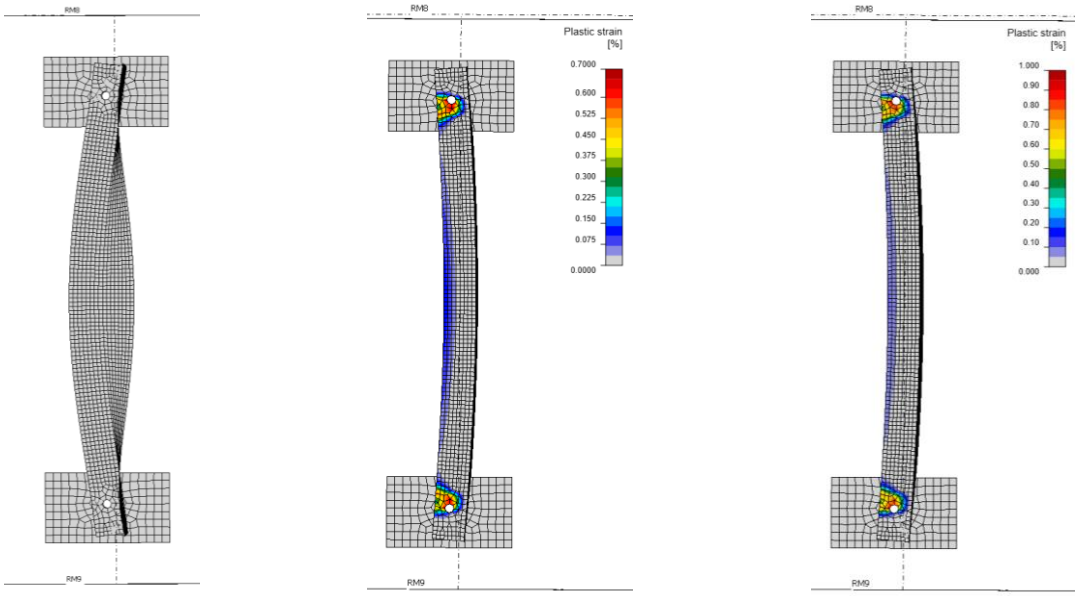

LBA	Imperfection: -1.1 mm	Imperfection: +1.1 mm
Mode 1	Resistance: 157.5 kN	Resistance: 162.4 kN
a)	b)	c)

Figure 5: Comparison between model with negative b) and positive c) imperfections

2.3. Selected benchmark case

As a benchmark case, the study of Unterweger and Taras [12] on the behaviour of hollow sections with slotted gusset plates is analysed in ABAQUS software package and reproduced with the software IDEA StatiCa. The system is composed of a steel member with a RHS 200/200/10 section without fillets and slotted gusset plates at each end that are welded to the profile. Dimensions of the plate are 750 mm x 260 mm. The corresponding geometry is shown in Figure

6. The length L_0 of the system was varied and two different boundary conditions were implemented at the supports. Axis I in Figure 6 along the edge of the gusset plate was either modelled as a hinge (BC1) or fully clamped (BC2). A thickness of t = 400 mm was used for the gusset plate. Dimensions of each system are listed in Table 2.

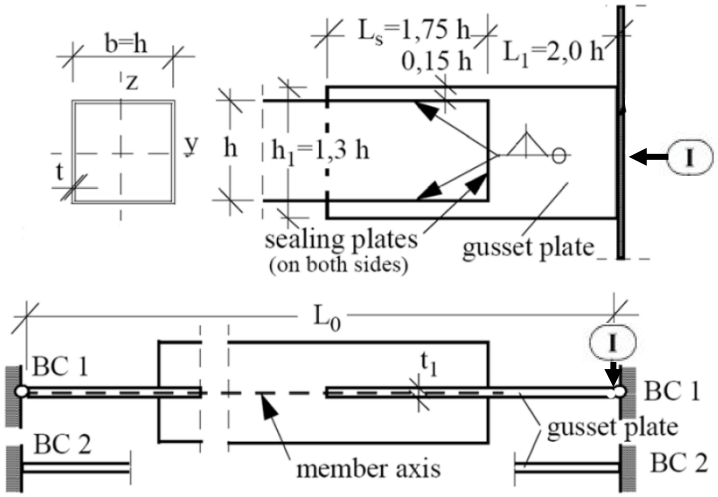

Figure 6: Geometry of modelled specimens from [12]

Table 2: Material properties used within investigations in [12]

Specimen	Support	L_0 [mm]
A	BC1	4000
B	BC1	8000
C	BC1	12000
D	BC2	4000
E	BC2	8000

The FE-model is composed of a combination of solid, shell, and beam elements. C3D8 solid elements were used for the gusset plate. The first 600 mm of the RHS was modelled with shell elements. Beam elements were used for the rest of the member and a rigid kinematic coupling was introduced between the shell and beam elements. A linear-elastic, ideal plastic material model was implemented to model a S235 steel. No strain hardening was considered. The same material parameters, as proposed in Table 15 before, were used in the framework of numerical simulations.

The simulation process was composed of two steps. As a first step, a LBA was performed to evaluate the eigenvalues as well as eigenshapes. Those shapes of symmetric and asymmetric buckling modes were used as initial imperfection shapes for GMNIA, applied in a further step. In the paper, different equivalent geometrical imperfections were used to scale the eigenmodes. Two cases were differentiated: an imperfection of the gusset plate of $L_{plate}/100$ based on EN ISO 13920 (1996) [5] and a maximum imperfection of $L_0/750$ according to EN 1090-2 (2008) [13]. The imperfection of the gusset plate accounts for an inclination $\varphi_{Max}=1/100$

from the fabrication process. The same imperfection amplitudes were used to allow a direct comparison of IDEA StatiCa with ABAQUS. A GMNIA was performed for the symmetric and asymmetric buckling modes, using successively both imperfections to scale the shapes of the eigenmodes, leading to four different ultimate loads for each system as summarized in Figure 7.

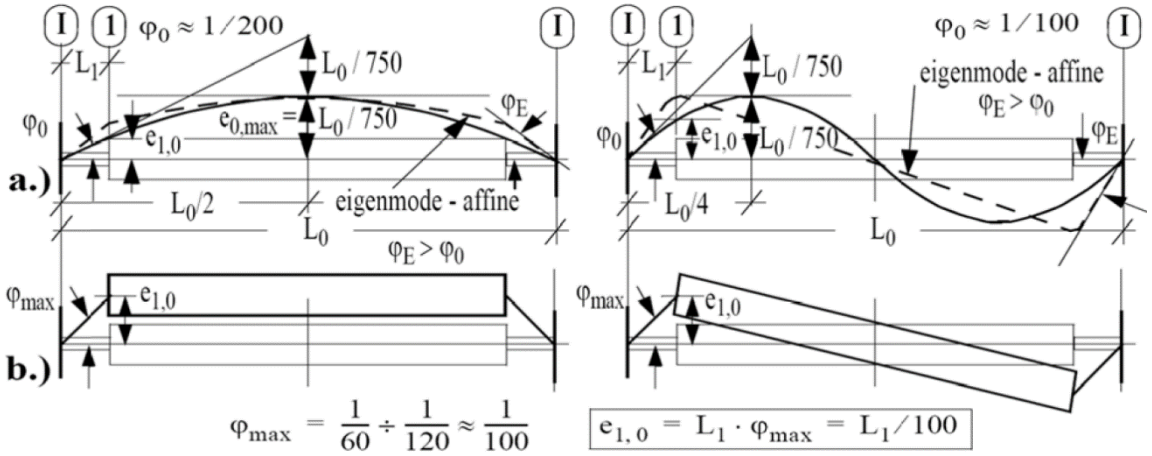

Figure 7: Imperfection assumptions, a) eigenmode-affine; b) gusset plate inclination, adopted from [12]

The five specimens are reproduced with IDEA StatiCa, a related member made with a plate with steel grade S355, and a cross-section of 200×200 mm is attached to the gusset plates. Both ends of the two related members are fixed, either displacements or rotations are constrained. The BC1 (hinge) is implemented by means of a one-sided weld with 10 mm throat thickness, while for the BC2 (fix) a butt-weld is modelled. Following the procedure presented in the previous chapter an MNA followed by a LBA is performed, the symmetric and asymmetric eigenmode are then amplified with an imperfection equal to the one of the paper of $L_0/750$. Figure 9 shows the comparison between the results with IDEA StatiCa and ABAQUS. Table 3 summarises the results with the respective imperfection implemented during the calculation.

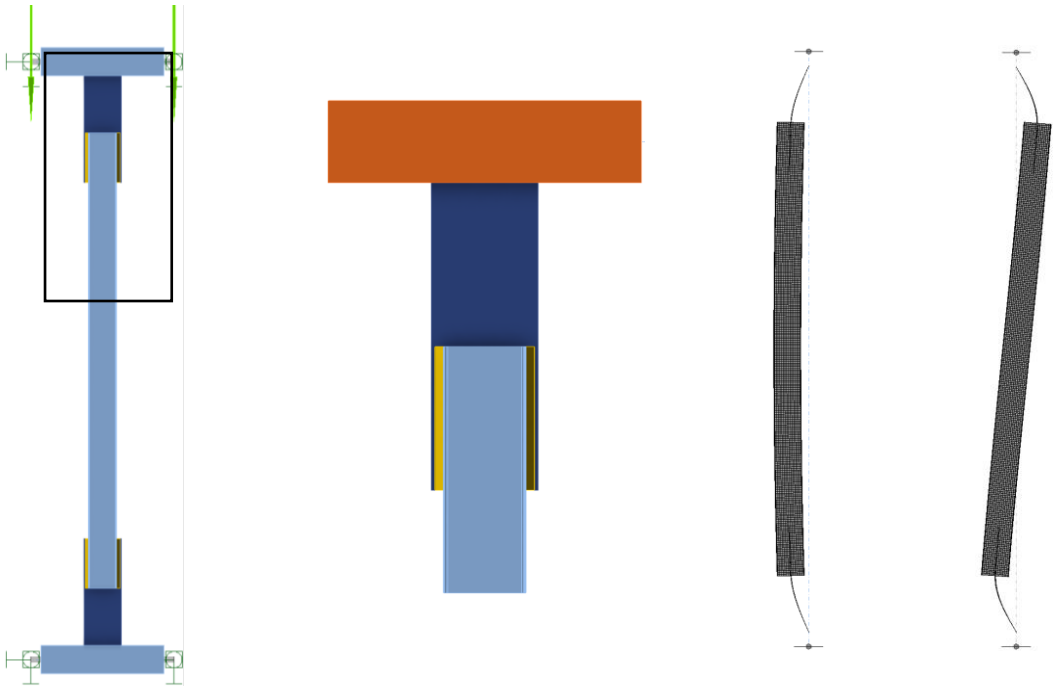

Figure 8: IDEA StatiCa Model of sample A [12] a) connection detail b), LBA results for symmetric c) and asymmetric mode d)

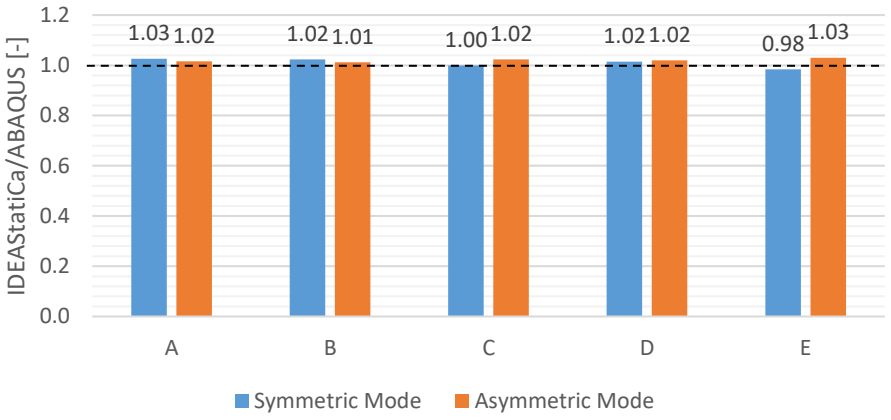

Figure 9: Comparison between the simulations in IDEA StatiCa and ABAQUS from [12]

Table 3: Summary of numerical results in Idea StatiCa and in ABAQUS from [12]

Specimens	A	B	C	D	E
Symmetric Mode					
ABAQUS [kN]	670	611	497	1386	1213
Idea StatiCa [kN]	687.2	625.3	496.8	1407.0	1193.6
Asymmetric Mode					
ABAQUS [kN]	707	514	430	1241	1086
Idea StatiCa [kN]	718.4	520.3	440.4	1266.0	1118.4
Imperfection amplitude [mm]	5.3	10.7	16.0	5.3	10.7

The results show good agreement with the load capacity difference only up to 3%. The differences may be attributed mainly to a different material model (no strain hardening in Abaqus and *E*/1000 in IDEA StatiCa), different meshing and other modelling strategies.

3. Proposed Method/Workflow

The proposed workflow is described throughout this section. It is limited to the standard case of one member/brace supported by two single-sided gusset plate connections at each end. Figure 8 gives a schematic outline of the overall system. The lengths of each element, i.e., either the gusset plate or the member, are denominated as L_g and L_c, respectively. The described workflow requires the calculation of an upper and lower limit for the local imperfections of the gusset plate, as well as the global imperfections of the member. Local gusset plate imperfection limits are chosen according to FprEN 1993-1-14 [4], providing the equivalent maximum imperfection $e_{g,max}$; and EN ISO 13920 [5], providing general tolerances for welded structures, leading to the minimum value $e_{g,min}$. Further, global imperfection boundaries for the member/brace are both ($e_{c,min}$ and $e_{c,max}$) defined according to FprEN 1993-1-14 [4]. Note that the Young's modulus has to be adjusted to $E = 200000\,\mathrm{N/mm^2}$ when using the formulations from FprEN 1993-1-14. Table 4 gives a summary of the used formulas, applied in the framework of the proposed method. Note that imperfection limits might be adjusted according to the used code provisions and project-related specifications.

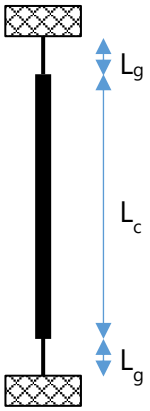

Figure 10: System with a column and two gusset plate connections

Table 4: Summary of imperfection for column and gusset-plate

	Limit column imperfection	**Limit gusset plate imperfection**
Maximum	$e_{c,max} = \alpha \cdot L_c/150$	$e_{g,max} = L_g/50$
Minimum	$e_{c,min} = L_c\ /\ 1000$	$e_{g,min} = L_g\ /\ 100$

The general procedure to determine the lowest resistance is summarised in Figure 11 and Figure 12. The first step requires a material non-linear analysis (MNA) as a first verification of the system, followed by a linear buckling analysis (LBA). The LBA provides the user with sorted

eigenmodes, starting with the lowest eigenvalue. The method distinguishes between two critical cases, see Figure 11, the symmetric (Case A) and the asymmetric (Case B) imperfection shape, which is often the critical, but in many cases neglected, failing mechanism. The reason for this is usually the fact that in many situations, this particular eigenmode is not the one with the lowest eigenvalue and, therefore, is not necessarily considered in the verification.

Case A requires the user to scale the shape of the symmetric eigenmode, as shown in Figure 11 a), so that the equivalent imperfection is the sum of the maximum column imperfection and the minimum gusset plate imperfection ($e_{\mathrm{A}} = e_{\mathrm{c,max}} + e_{\mathrm{g,min}}$). Case B, on the other hand, requires the user to scale the shape of the asymmetric eigenmode, as shown in Figure 11 (b), so that the equivalent imperfection is equal to the sum of the maximum gusset plate imperfection and the minimum column imperfection ($e_B = e_{g,max} + e_{c,min}$). Note that for both cases, two calculations have to be performed, since the imperfection in IDEA StatiCa can be implemented either with a positive or negative sign. The smallest resistance value from the four simulations is subsequently the determinant resistance of the member.

a) b)

Figure 11: Imperfections for symmetric modes a) and asymmetric modes b)

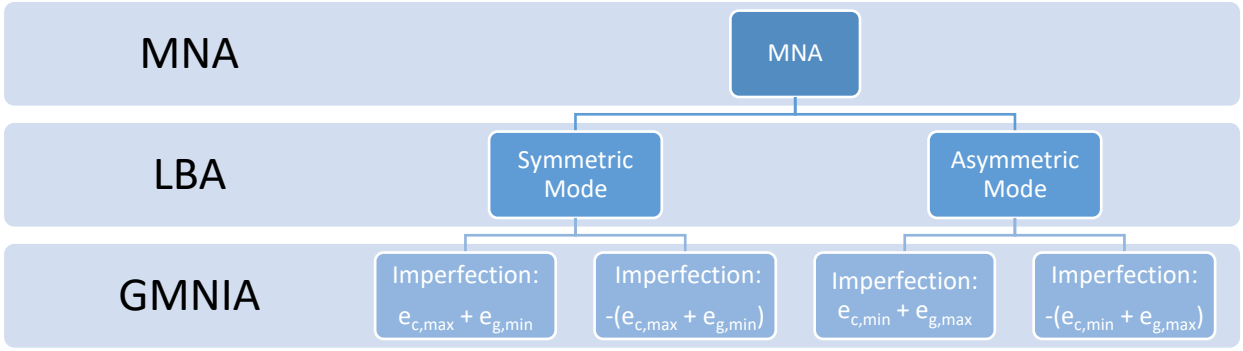

Figure 12: Flowchart of imperfection settings

Note that in some cases local buckling might be the driving failing scenario. Dependent on the global slenderness of the member and the thickness of the gusset plates, i.e., the distribution of stiffnesses in the system, local buckling modes might appear decisive according to the lowest eigenvalue. In [14] and [11], a detailed comparison of the local and global buckling behavior, as well as their combination, is presented for different profiles and member lengths along with a developed workflow. In a condensed formulation, the following limits can be used for better categorization in the first step. Global buckling might be neglected if $\alpha_{cr} \geq 25$, where $\alpha_{cr} = 1/\lambda_{glob}^2$. Local buckling might be neglected if $\alpha_{cr} \geq 2.2$, where $\alpha_{cr} = 1/\lambda_{loc}^2$.

4. Comparison

4.1. Experimental Tests

The experimental database is gathered from the literature; it includes the results from **25 experimental tests** in total. All experimental results are summarised with additional information on geometry and material properties. Each test specimen was performed using the software package IDEA StatiCa Member. By following the workflow presented in Section 0, the determinant resistances for Symmetric and Asymmetric modes were computed, and the results are presented and compared to the experimental results for each test in the following sections.

4.1.1. J. Vesecky, K. Cabova and M. Jandera [15]

Results of **6 full-scale tests** were published by Vesecký et al. [15], which investigate the behaviour of bracings composed of CHS member with gusset plate connections on both sides. An example of a test specimen is shown in Figure 13 [15]. The used profile is a CHS102/4 cross-section, with a diameter of 102 mm and the thickness of 4 mm. Each end connection consists of a gusset plate assembled to a cleat plate with different M20 8.8 bolts configuration; see Figure 13.

Figure 13: Test specimen C2 and different end-plate constellations adopted from [15]

Two types of specimens were tested (see Figure 14): *(i)* type C with perpendicular end of gusset plate and; *(ii)* type D with oblique end of gusset plate. The specimens were made from steel grade S355. Table 5 summarizes the specimens used, their corresponding dimensions, and the number of bolts at the gusset-plate connection. All experimental tests were performed for the load case of pure compression.

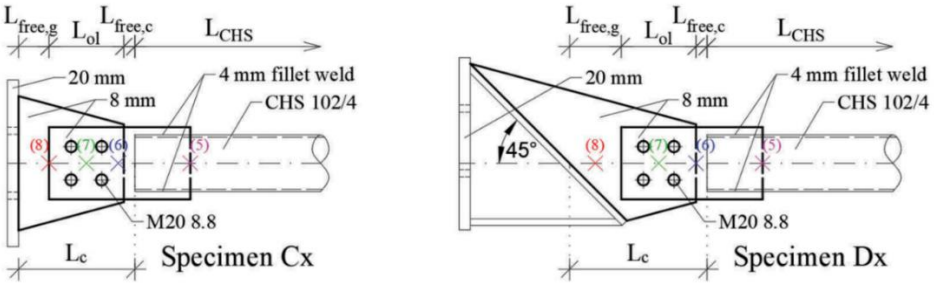

Figure 14: Specimen type C (left) and D (right) from [15]

Table 5: Geometry of the tested specimen, adopted from [15]

Specimen	α [°]	L_c [mm]	L_{ol} [mm]	$L_{free,g}$ [mm]	$L_{free,c}$ [mm]	L_{CHS} [mm]	Bolts
C1	90	210	135	55	20	2000	4
C2	90	245	170	55	20	2000	2
C3	90	210	170	20	20	2000	2
D1	45	248	135	93	20	2000	4
D2	45	298	135	143	20	2000	4
D4	45	333	170	143	20	2000	2

Tensile tests were performed for the gusset plate (three tests) and the CHS102/4 profile (two tests) to evaluate the real material properties. Those results are summarized as average values in Table 6.

Table 6: Average material properties obtained from tensile coupon tests

Component	t [mm]	E [MPa]	f_y [MPa]	f_u [MPa]	A [%]
Gusset plate	8.05	199’900	405.0	610.9	24.2
CHS 102/4	3.65	201’100	358.2	598.4	23.0

All six specimens tested by Vesecký et al. [15] are modelled with IDEA StatiCa as for the benchmark case presented in Section 2.3. A related member is attached to the gusset plate with a butt weld, as shown in Figure 15. The symmetric and asymmetric eigenmodes are amplified by the imperfection summarised in Table 7. For specimens D1, D2, and D4, a strain limit of 15% was used to allow for more deformation and simulate behavior consistent with experimental observations.

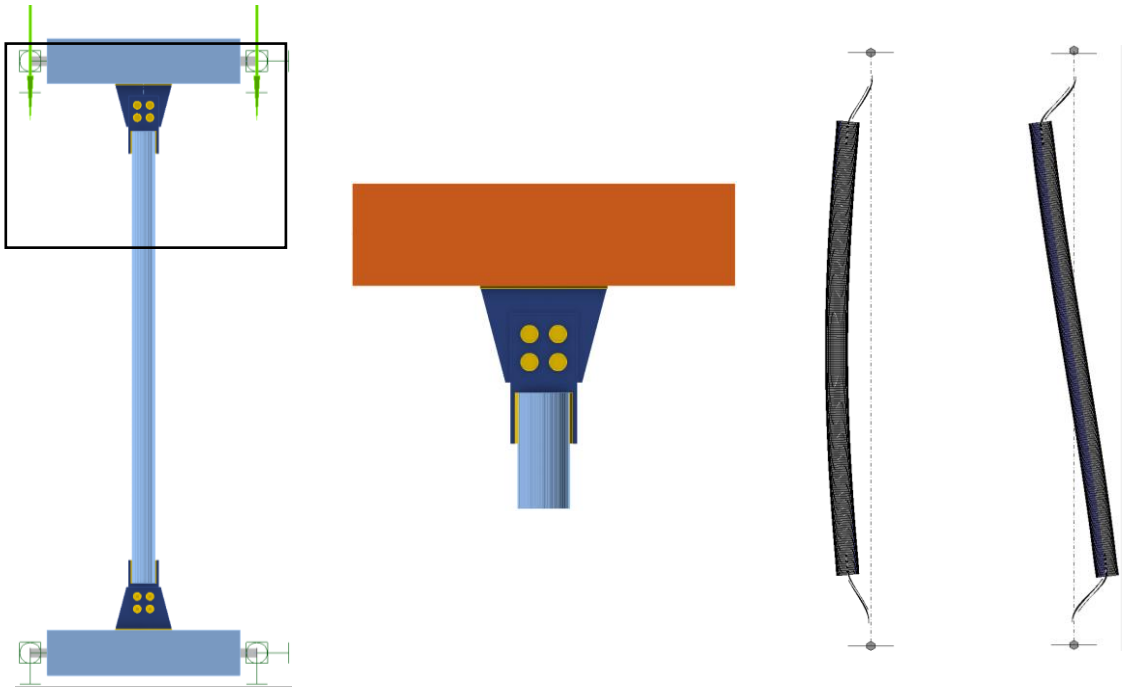

a) b) c) d)

Figure 15: IDEA StatiCa Model of sample C1 [15] a) connection detail, b) LBA results for symmetric c) and asymmetric mode d)

From the results shown in Figure 16, it is clear that the determinant mode is the asymmetric one, as was the case also in the experimental campaign. Indeed, the resistances from the numerical simulations for mode 2 are always smaller. The numerical simulations provide slightly lower load resistances than the experiment except for specimens C1, D1, and D4, which are slightly higher, proving that IDEA StatiCa can conservatively estimate the failure mode and the resistance of such samples.

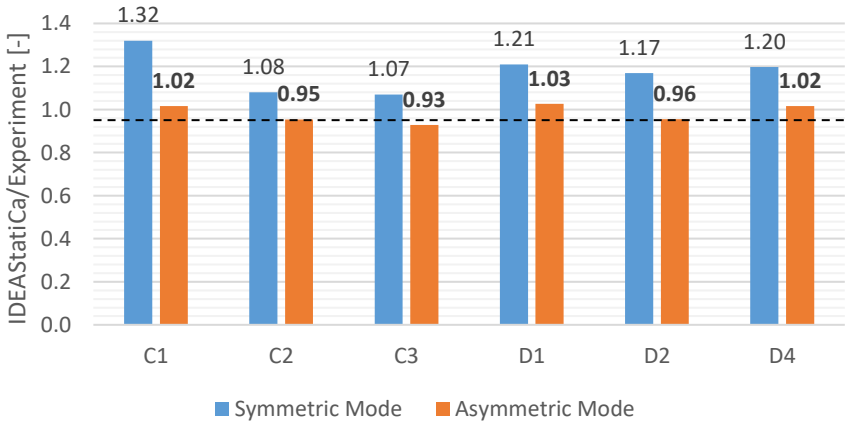

Figure 16: Comparison between GMNIA simulations and physical tests from [15]

Table 7: Summary of experimental and numerical results [15]

Specimens	C1	C2	C3	D1	D2	D4
Experiment [kN]	106.2	93.3	112.5	102.8	101.7	92.1
Symmetric mode						
Numerical IDEA StatiCa [kN]	140.1	100.8	120.3	124.4	119.0	110.3
Imperfection amplification [mm]	4.90	5.25	4.90	5.28	5.78	6.13
Asymmetric Mode						
Numerical IDEA StatiCa [kN]	107.9	89.0	104.4	105.5	97.2	93.6
Imperfection amplification [mm]	6.20	6.90	6.20	6.96	7.96	8.66

4.1.2. X. Khoo, M. Perera and F. Albermani [16]

12 full-scale tests using different member lengths and eccentric cleats were published by Khoo et al. [16]. The geometry of the connections and the test setup are shown in Figure 17. The corresponding dimensions of the specimens can be found in Table 8. The members are made of hot-rolled CHS 139,7/3,5 profiles. The connections at both ends consist of a cleat and a gusset plate bolted together. All the cleats were assembled using 4 M20 snug-tight bolts. Spacings are 70 mm in the horizontal direction (S_p) and 110 mm in the vertical direction (S_g). The distance from the edge (A_e) is equal to 35 mm. Cleat and gusset plate have a thickness of 10 mm. Two different types of steel grades were used for connection and member. Additionally, 2 coupon tests were conducted for the CHS sections and 4 coupon tests for the cleat plates to measure the effective yield strength ($f_{y,Test}$). The average values for the material properties, as well as test results are listed in Table 9 below.

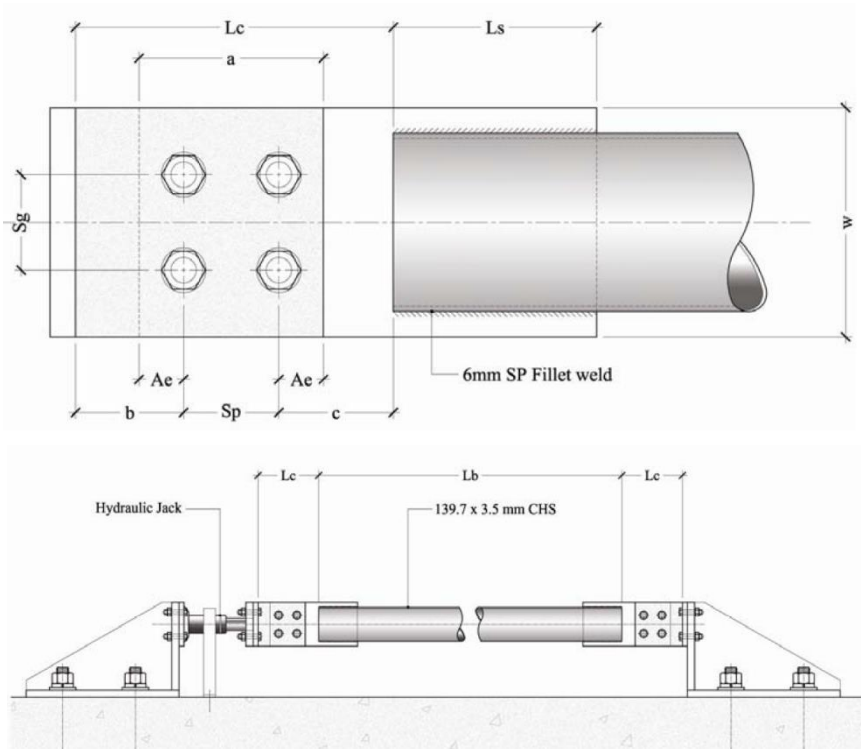

Figure 17: Geometry of the connection and test setup [16]

Table 8: Dimensions of investigated test specimens [16]

Specimen	L_b [mm]	L_c [mm]	b [mm]	w [mm]	a [mm]	c [mm]	L_s [mm]
A1	3000	170	50	180	140	50	260
A2	3000	170	50				
A3	3000	170	50				
B1	4000	170	50				
B2	4000	220	100				
B3	4000	270	150				
C1	5000	170	50				
C2	5000	220	100				
C3	5000	270	150				
D1	6500	170	50				
D2	6500	170	50				
D3	6500	170	50				

Table 9: Material properties of the specimens derived from coupon tests [16]

Element	Material	f_y [MPa]	f_u [MPa]	$f_{y,Test}$ [MPa]
CHS 139.7/3.5	Steel Grade 350	360	450	345
Connection	Steel Grade 300	310	430	320

The 12 specimens were modelled using the software package IDEA StatiCa Member. Note that the specimens A1, A2, and A3 were identical. Therefore, one numerical simulation was performed and compared to the results of tests A1 to A3. The same procedure applies for specimens D1, D2, and D3, leading to 8 numerical simulations for 12 physical test results. The same procedure as for the previous experimental comparison was used with a plate with the cross-section of 200x200 mm as a related member with butt weld; as an example, Figure 18 shows the model of sample A2.

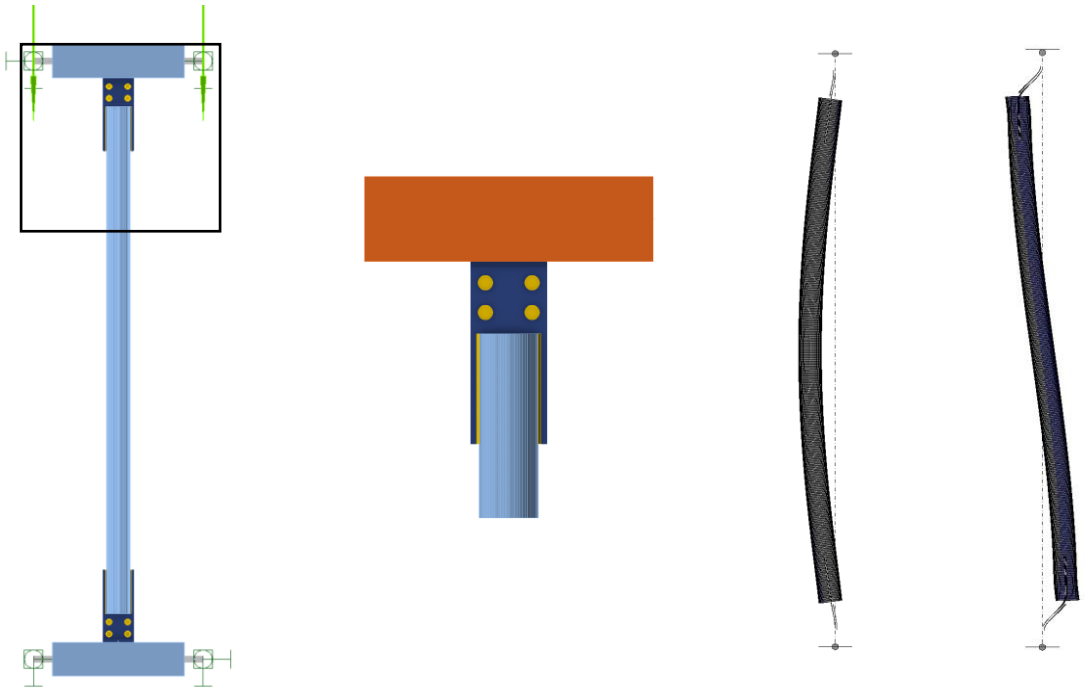

Figure 18: a) IDEA StatiCa Model of sample A2 [16], b) connection detail, LBA results for c) symmetric and d) asymmetric mode

Figure 19 shows the results of the comparison between numerical and experimental. The asymmetric mode is determinant for all specimens except for the last three: D1, D2, and D3. The detailed results and the imperfection implemented are summarised in Table 10. As for the previous paper, IDEA StatiCa is able to safely determine the resistances of the members with small error, with the only exception for sample D2, where the resistance is slightly overestimated by 2%.

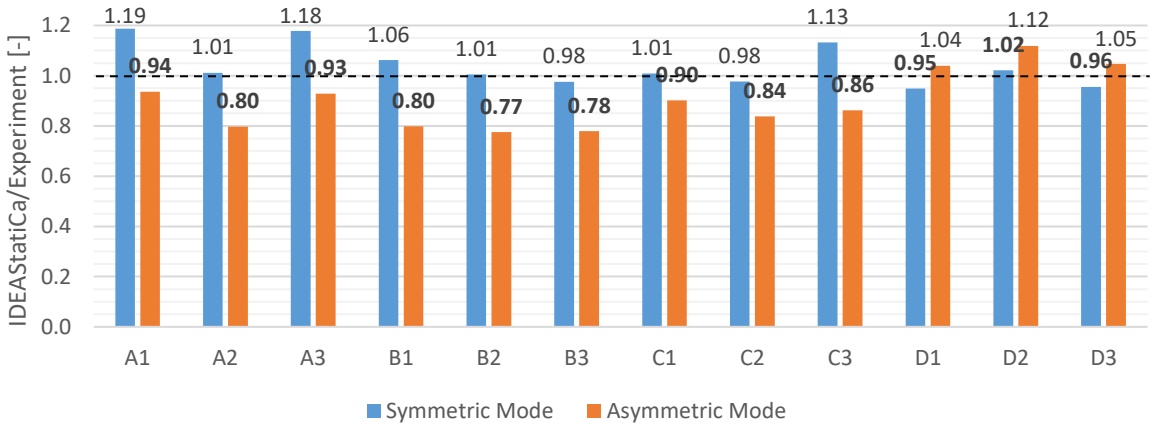

Figure 19: Comparison between IDEA StatiCa Member simulations and experimental results from [16]

Table 10: Summary of experimental [16] and numerical results from IDEA StatiCa

Specimens	A1	A2	A3	B1	B2	B3	C1	C2	C3	D1	D2	D3
Experiment [kN]	158.5	186.1	159.8	175.1	155.4	131.4	165.3	153.0	115.5	141.0	131.0	140.0
Symmetric Mode												
IDEA StatiCa [kN]		188.2		186.0	156.2	128.2	166.8	149.4	130.8		133.8	
Imperfection amplitude [mm]		5.9		7.3	7.8	8.3	8.7	9.2	9.7		10.8	
Asymmetric Mode												
IDEA StatiCa [kN]		148.4		139.8	120.4	102.4	149.1	128.3	99.5		146.6	
Imperfection amplitude [mm]		6.4		7.4	8.4	9.4	8.4	9.4	10.4		9.9	

4.1.3. M. Kettler, L. Gerit, H. Unterweger [17]

A total of 27 experimental tests on bolted steel angles with varying end support conditions were conducted at Graz University of Technology by Kettler et al. [17]. 14 specimens were produced with two-bolt connections and 13 with one-bolt connections; therefore, 27 full-scale tests in total. 24 specimens were made of the European hot-rolled section L80×8 and 3 specimens with two-bolt connections were fabricated with the larger L120×12 section. All profiles are bolted to a plate with a thickness of 25 mm, as shown in Figure 20. Due to the thick gusset plate, only limited interactions with the member were observed. In addition, some of these tests were already reproduced with IDEA StatiCa in [18]. Therefore, 12 selected L80×8 profiles are modelled using CBFEM.

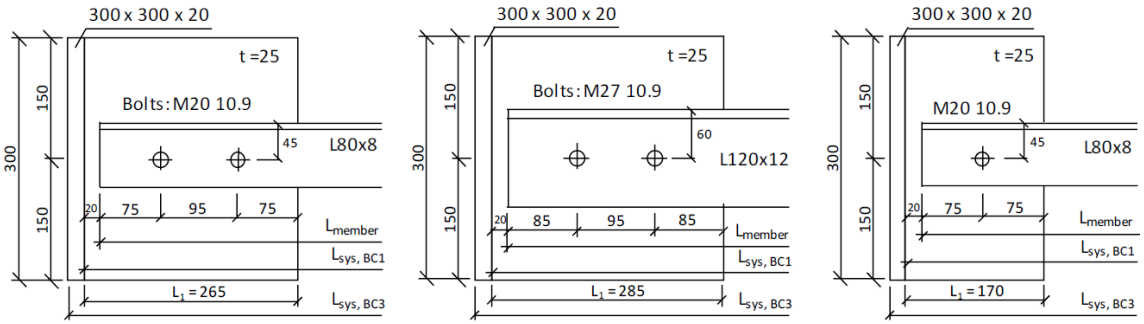

Figure 20: Details of studied bolted connections from [17]

Table 11: Dimensions of the tested L80×8 profiles from [17]

Specimen	Bolts	Supports	L_{member} [mm]	L_{System} [mm]	b_{mean} [mm]	t_{mean} [mm]
B4	1×M20 10.9	BC1	1140	1180	79.4	7.8
B5	1×M20 10.9	BC1	1820	1860	79.5	7.8
C1	1×M20 10.9	BC1	3170	3210	79.4	7.8
D1[1]	2×M20 10.9	BC1	1140	1180	79.4	7.8
D2[1]	2×M20 10.9	BC1	2630	2670	79.5	7.9
D3[1]	1×M20 10.9	BC1	1140	1180	79.5	7.8
D4[1]	1×M20 10.9	BC1	3170	3210	79.4	7.9

[1]: bolts were not preloaded, but only hand-tight

For the L80×8 sections, M20 bolts of grade 10.9 were used, while M27 bolts of grade 10.9 were employed for the L120×12 sections. The bolts of four tests have been hand-tight and all other bolts were preloaded. Three different boundary conditions were used throughout the test: clamped support (BC1), knife edge support that only allows rotation about the axis parallel to the connected leg (BC2), and fully hinged support with only the rotation about the longitudinal axis being restrained (BC3). The real cross-sectional dimensions of each specimen were measured (b_{mean} & t_{mean}). The dimensions of the tested L80×8 specimens are listed in Table 12. In addition, material tests have been conducted to measure the yield strength $f_{y,mean}$, ultimate strength $f_{u,mean}$, and the modulus of elasticity E_{mean}. Results are presented in Table 12. Finally, the specimens were placed in a test setup shown in Figure 21, where a normal force was applied through a hydraulic jack.

Table 12: Material properties of the tested L80×8 profile from [17]

Specimen	$f_{y,mean}$ [MPa]	$f_{u,mean}$ [MPa]	E_{mean} [MPa]
B4	326.8	467.4	199 458
B5	326.8	467.4	209 284
C1	333.9	469.2	209 284
D1, D2, D3, D4	322.4	463.0	194 818

Figure 21: Test setup from [17]

Seven models reproducing the specimens were built in IDEA StatiCa; the related members at each end are 200×200mm steel plates. All bolts are modelled as preloaded with a force transmission through friction. Prestressing force is $F_{pr,t} = k \cdot f_{ub} \cdot A_s$ with the factor k equal to 0.7 as a default setting. Figure 22 shows an example of the model.

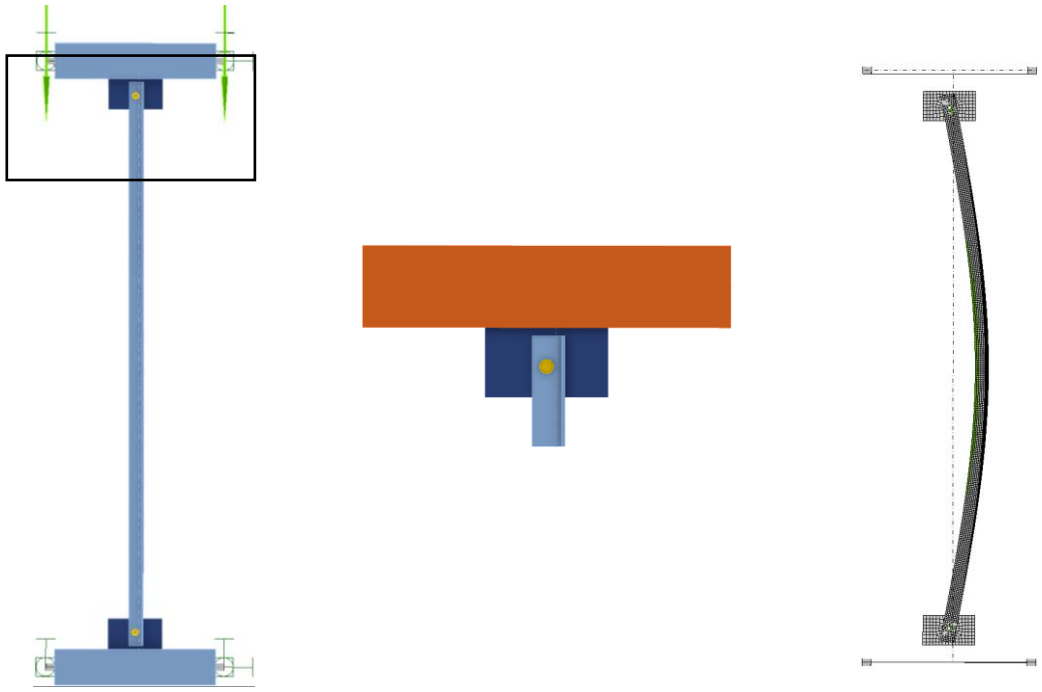

Figure 22: a) IDEA StatiCa Model of sample C1 [17], b) connection detail, and c) LBA results for symmetric mode

For this specific case, only the symmetric mode is analysed since all other modes are global buckling. Since the gusset plates of samples B4, B5, C1, D3, and D4 are connected to the column only by one bolt, the imperfection amplitude applied could be assumed to be smaller. The imperfection of the gusset plate could be neglected due to the fact that the deformation shape (see Figure 22) does not include the gusset plate; the column rotates around the bolt. The formula presented in Section 0 can be simplified as follows for the aforementioned cases:

$$e_A = e_{c,max} + \cancel{e_{g,min}} = e_{c,min}$$

The comparison of the results obtained with the GMNIA and the experimental results from the physical tests are shown in Figure 23. In Table 13, the numerical and experimental values, as well as the used imperfections, are summarised.

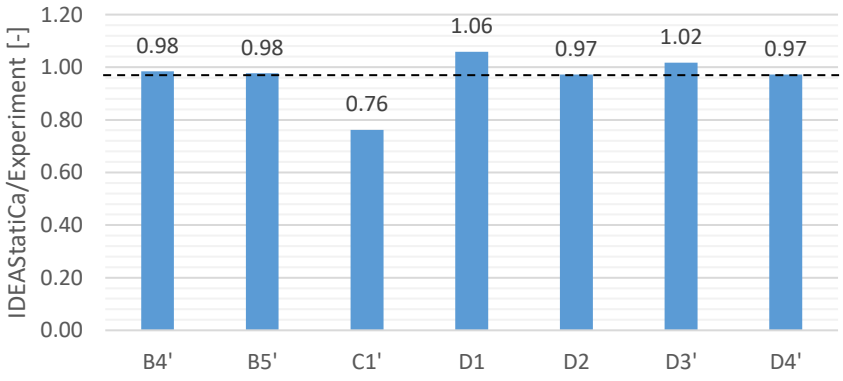

Figure 23: Comparison between IDEA StatiCa Member simulations and physical tests from [17]

Table 13: Summary of experimental [17] and numerical results

Specimens	B4	B5	C1	D1	D2	D3	D4
Experiment [kN]	162.9	132.1	98.4	260.2	177.5	154.8	73.1
Symmetric mode							
IDEA StatiCa [kN]	151.9	115.4	64.7	275.5	172.6	149.8	60.9
Imperfection amplitude [mm]	1.1	1.8	3.2	6.4	11.2	1.1	3.2

4.2. Numerical Tests

Analogously to the experimental tests, an additional numerical study is compared with numerical models made with the software package IDEA StatiCa Member. By following the workflow presented in Section 0, the determinant resistance for Symmetric and Antisymmetric modes were computed, and the results are presented and compared in the following sections.

4.2.1. H. Unterweger, R. Ofner [19]

Unterweger and Ofner [19] published the results of 24 numerical simulations for hollow sections performed with the FE-program ABAQUS [20]. The system is composed of a steel member with an RHS 100/100/5 section without fillets and slotted gusset plate connections at the end. These are composed of two plates welded together. Dimensions are 250 mm × 130 mm for the first plate (KB1) and 330 mm × 100 mm for the second plate (KB2). The corresponding geometry is shown in Figure 24.

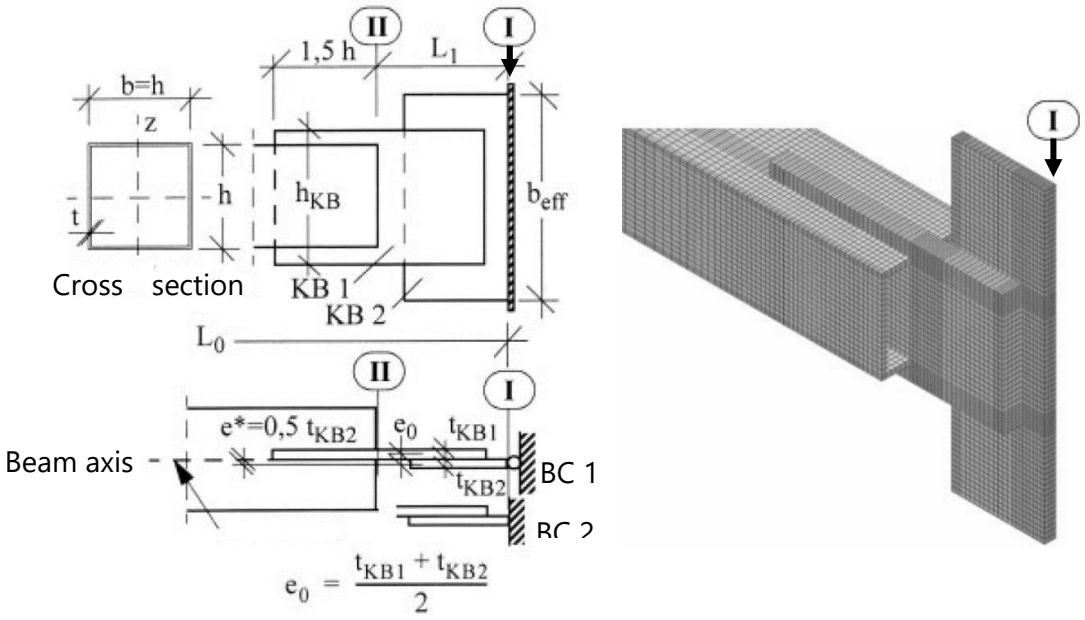

Figure 24: Geometry and FE-model [19]

Three parameters were varied: length of the member L_0, thicknesses of the plates at the connection (t_{KB1} & t_{KB2}), and support conditions. The different lengths of the RHS profile were 2 000,

4 000, 6 000, and 8 000 mm. A thickness of 12 mm or 20 mm was used for the gusset plates. Two different boundary conditions were implemented at the supports. Axis I along the edge of KB2 was either modelled as a hinge (BC1) or clamped (BC2), as shown in Figure 24. The different combinations are numbered from A1 to L2. Dimensions of each system are listed in Table 14.

Table 14: Specimens investigated in [19]

t_{KB1}/t_{KB2}	Supports	L_0 [mm]			
		2000	4000	6000	8000
12/12	BC1	A1	B1	C1	D1
	BC2	A2	B2	C2	D2
20/20	BC1	E1	F1	G1	H1
	BC2	E2	F2	G2	H2
20/21	BC1	I1	J1	K1	L1
	BC2	I2	J2	K2	L2
Fixed dimensions: h = 100 mm, L_1 = 125 mm, h_{KB} = 130 mm & b_{eff} = 330 mm					

The FE-model is composed of a combination of solid and beam elements. To accurately model the behaviour at the connections, the plates and the first 500 mm of the RHS section are modelled with solid elements. The rest of the member is made of beam elements. A symmetry condition was implemented to model half of the system to reduce computational costs. A linear-elastic, ideal-plastic material model without a strain hardening modulus was used within the FE model. Steel grade S235 was used throughout the numerical simulations. The influence of residual stresses was neglected. The yield strength f_y, elastic modulus E, and Poisson's ratio ν are listed in Table 15. The imperfection amplitude applied for the GMNIA in the FE model was set to a value equal to $e = L_0/1000$.

Table 15: Material properties used within investigations in [19]

f_y [MPa]	E [MPa]	ν [-]
235	210 000	0.3

The comparison to the ABAQUS results of the 24 models with the software IDEA StatiCa are presented in Figure 26. The boundary conditions are carefully implemented similarly to the benchmark case, namely a butt weld for fix boundary and a one-sided filler weld for the case of the hinge. The model is shown in Figure 25:

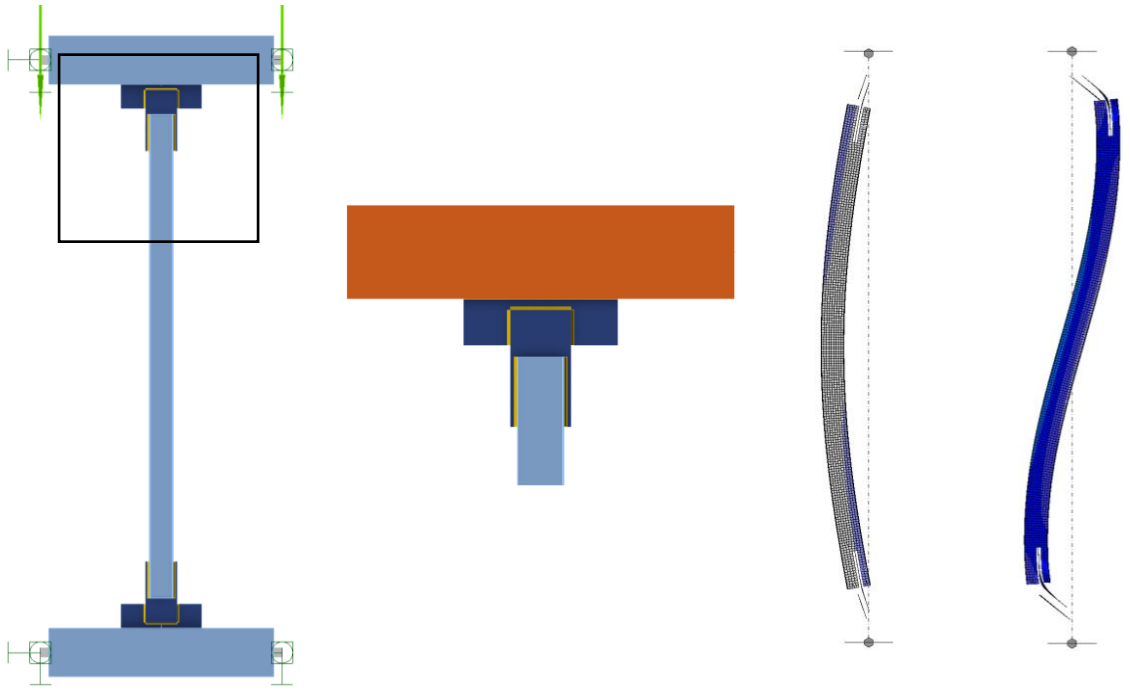

Figure 25: a) IDEA StatiCa Model of sample E1 [19], b) connection detail, LBA results for c) symmetric and d) asymmetric mode

Both modes, symmetric and asymmetric, are analysed, and the exact value of the resistance as well as the imperfection implemented in the GMNIA calculation are summarized in Table 16. The determinant mode for samples A1-F1, I1-J1, and A2 is the asymmetric one, while for all other cases, the load resistance for the symmetric one is smaller.

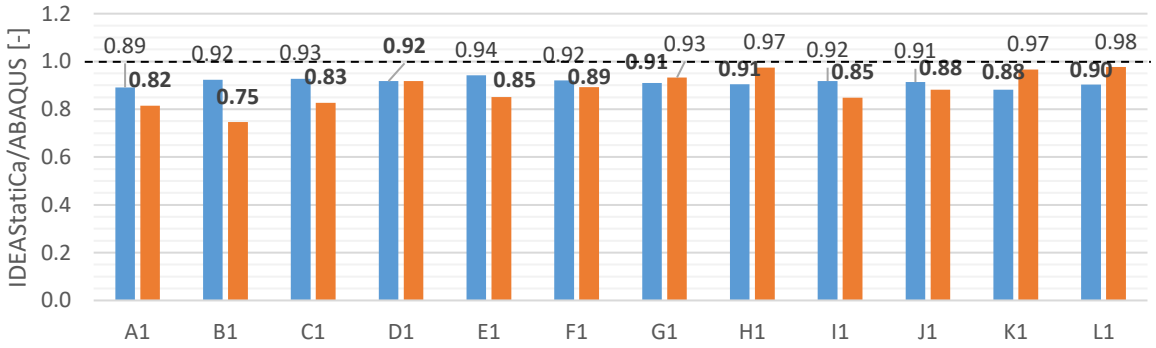

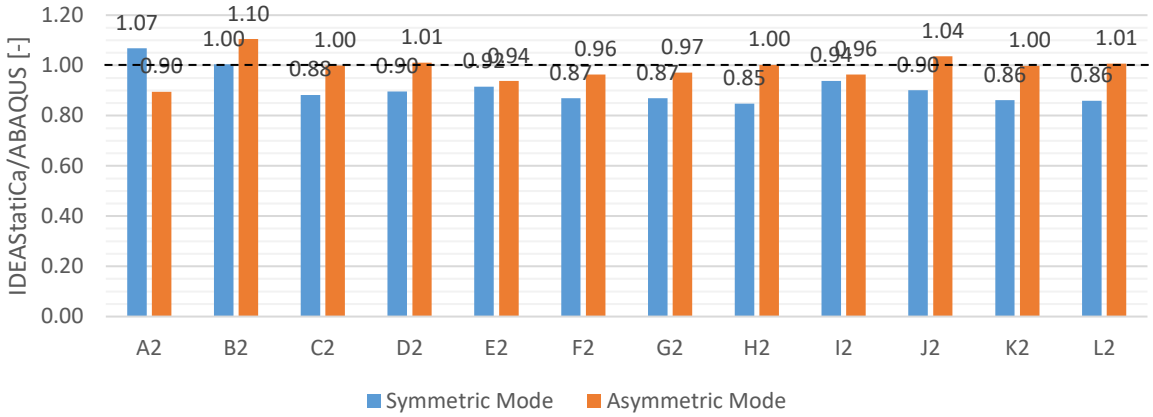

Figure 26: Comparison between the numerical results from IDEA StatiCa and from ABAQUS [19]

Table 16: Summary of numerical results in IDEA StatiCa and in ABAQUS from [19]

Specimens	**A1**	**B1**	**C1**	**D1**	**E1**	**F1**	**G1**	**H1**	**I1**	**J1**	**K1**	**L1**
ABAQUS [kN]	71.9	72.8	71.4	66.1	138.0	134.8	121.4	79.0	163.9	159.4	131.7	81.7
Symmetric mode												
IDEA StatiCa [kN]	64.1	67.2	66.2	60.6	130.1	124.2	110.5	71.5	150.5	145.6	116.1	73.8
Imperfection amplitude [mm]	3.9	6.7	9.5	12.3	3.9	6.7	9.5	12.3	3.9	6.7	9.5	12.3
Asymmetric mode												
IDEA StatiCa [kN]	58.6	54.3	59.0	60.6	117.4	120.3	113.3	77.0	139.1	140.6	127.3	79.8
Imperfection amplitude [mm]	4.4	6.4	8.4	10.4	4.4	6.4	8.4	10.4	4.4	6.4	8.4	10.4

Specimens	**A2**	**B2**	**C2**	**D2**	**E2**	**F2**	**G2**	**H2**	**I2**	**J2**	**K2**	**L2**
ABAQUS [kN]	234.9	234.4	161.2	97.8	368.4	292.0	189.8	127.7	287.1	287.1	189.3	122.8
Symmetric mode												
IDEA StatiCa [kN]	250.9	235.5	142.2	87.6	337.3	253.8	165.0	108.2	269.4	258.9	163.2	105.6
Imperfection amplitude [mm]	3.9	6.7	9.5	12.3	3.9	6.7	9.5	12.3	3.9	6.7	9.5	12.3
Asymmetric mode												
IDEA StatiCa [kN]	210.3	258.9	161.0	98.9	345.4	281.3	184.4	128.0	276.6	297.6	189.0	123.6
Imperfection amplitude [mm]	4.4	6.4	8.4	10.4	4.4	6.4	8.4	10.4	4.4	6.4	8.4	10.4

IDEA StatiCa Member provides in all cases smaller load resistance than the Abaqus model. The reason for that is primarily higher imperfection amplitudes.

5. Conclusions

In this report, comparisons were made between calculations in IDEA StatiCa Member and experimental and numerical results from the literature. The aim was to derive a practice-oriented procedure for the application of imperfection amplitudes and shapes within GMNIA simula-

tions. In the first step, numerical results from Unterweger and Taras [12] were taken for a benchmark case (see Section 2.3) to underline model approaches and an overall comparability between IDEA StatiCa and Abaqus. By using the same imperfection assumptions as proposed in [12], it was possible to reproduce the same load-bearing capacities. Deviations between the performed GMNIA simulations are at most $\pm 3\%$. This level of deviation is common and well within the range of acceptability. IDEA StatiCa Member is able to provide comparable predictions for this phenomenon as general-purpose finite element software, Abaqus.

Further, experimental results and numerical simulations collected from the literature ([15], [16], [17] and [19]) were compared through GMNIA simulations in IDEA StatiCa Member by using the proposed imperfection shapes and amplitudes from the presented workflow in Section 3. In general, for members in compression with gusset plate connections, four imperfection shapes should be tested:

- $e_{\mathrm{A}} = e_{c,max} + e_{g,min}$
- $e_B = e_{g,max} + e_{c,min}$
- both with plus and minus signs,

where $e_{c,max} = \alpha \cdot L_c/150$, $e_{g,max} = L_g/50$, $e_{c,min} = L_c\ /\ 1000$, $e_{g,min} = L_g\ /\ 100$, α is the column imperfection factor, L_g is the length of the gusset plate, and L_c is the column length.

In almost all cases, the results were on the safe side. Some calculations lead to a slight overestimation of the load-bearing capacity by around 2%. The vast majority of the calculations within this report emphasize that *(i)*: there is a noticeable difference in the achieved capacities when using the symmetrical or the asymmetrical mode as the imperfection shape and, *(ii)*: the asymmetric imperfection shape often leads to lower capacities achieved by the system within the considered cases. Note that some experiments were designed in such a way that gusset plate buckling was the governing failing criterion.

The analysis revealed that, in certain scenarios, applying gusset plate imperfections is not practically necessary and may lead to an overloading of the system. As discussed in Section 4.1.3, the gusset plates in samples B4, B5, C1, D3, and D4 are connected to the column with a single bolt at each end, effectively creating a "pinned connection" in simplified terms. Since the imperfection shape derived from the linear buckling analysis (LBA) (see Figure 22) does not explicitly include the gusset plate, the local imperfection amplitude can reasonably be disregarded.

Conversely, depending on the local and global slenderness, situations may arise where local buckling in the member becomes critical. This is particularly evident in the LBA analysis, where local buckling-related modes (short-wavelength imperfections in the member) appear within the first eigenmodes, with α_{cr} values dropping below 2.2. For further details, the reader is kindly referred to [14] and [11].

A final point to address is the selection of the plastic strain limit (see Section 4.1.1). A plastic strain limit of 15% was selected for direct comparisons with the experiments to accurately capture the observed buckling behavior. However, for design models, a more conservative plastic strain limit of 5% is recommended to incorporate an additional margin of safety.

6. References

[1] "Bahnhof Bern: Das längste Perron der Schweiz', Baublatt," [Online]. Available: https://www.baublatt.ch/baupraxis/bahnhof-bern-das-laengste-perron-der-schweiz. [Accessed 13 July 2023].

[2] H. Schmidt, M. Fastabend, P. Swadlo and H.-G. Lommen, "Ein ungewöhnliches Stabilitätsproblem verursacht Schadensfall," *Stahlbau,* vol. 77, no. 142, p. 862–869, 2008.

[3] U. H and T. A, "Compression Member with Hollow Sections and COncentric Slotted Gusset Plates - Behaviour and Recommendation Design Model," *Proceedings of the Annual Stability Conference Structural Stability Research Council,* pp. 19-34, April 2013.

[4] *Eurocode 3: Design of steel structures - Part 1-14: Design assisted by FEM,* Draft Version - January 2022.

[5] DIN Deutches Institut für Normung, *DIN EN ISO 13920:1996-11 Schweissen - Allgemeintoleranzen für Schweisskonstruktionen - Längen und Winkelmasse, Form und Lage.*

[6] DIN EN Duetsches Institut für Normung, *Eurocode 3 - Bemessung und Konstruktion von Stahlbauten - Teil 1-5: Plattenförmige Bauteile; Deutsche Fassung EN 1993-1-5:2006,* 2006.

[7] *Eurocode 3: Design of steel structures - Part 1-1: General rules and rules for buildings,* August 2020.

[8] L. J, "Additional investigations concerning initial bow imperfections for flexural buckling according to Eurocode 3 Part 1-1," *ce/paper,* vol. 1, no. 5-6, pp. 35-42, 2017.

[9] L. J, "Repräsentative Vorkrümmungen e0 für das Biegeknicken–Ergänzende Untersuchungen," *Stahlbau,* vol. 86, no. 8, pp. 707-715, 2017.

[10] W. F, "Design of steel and stainless steel structures by advanced inelastic analy-sis," *Doctoral Thesis, Imperial College London,* 2019.

[11] T. A and M. A, "IDEA StatiCa Member, WP1-2: Comparison of the Buckling Resistance of I-shaped cross-sections. Chair of Steel and Composite Structures, ETH Zurich.," IDEA

StatiCa, 2021. [Online]. Available: https://www.ideastatica.com/support-center/comparison-of-buckling-resistance-of-i-shaped-cross-sections.

[12] H. Unterweger and A. Taras, "Compression Members with Hollow Sections and Concentric Slotted Gusset Plates – Behavior and Recommended Design Model," *Proceedings of the Annual Stability Conference Structural Stability Research Council,* pp. 19-34, April 2013.

[13] DIN EN Deutches Institut für Normung, *Ausführung von Stahltragwerken und Aluminiumtragwerken - Teil 2: Technische Regeln für die Ausführung von Stahltragwerken; Deutsche Fassung EN 1090-2:2018,* September 2008.

[14] T. A and M. A, "IDEA StatiCa Member, WP1-1: Comparison of the Buckling Resistance of SHS and RHS Profiles. Chair of Steel and Composite Structures, ETH Zurich," ODEA StatiCa, 2021. [Online]. Available: https://www.ideastatica.com/support-center/comparison-of-the-buckling-resistance-of-shs-and-rhs-profiles.

[15] J. Vesecky, K. Cabova and M. Jandera, "Tests of gusset plate connection under compression," *Proceedings of the international colloquia on stability and ductility of steel structures,* pp. 1218-1226, 11-13 September 2019.

[16] X. Khoo, M. Perera and F. Albermani, "Design of eccentrically connected cleat plates under compression," *Advanced Steel Construction Vol. 6, No. 2,* pp. 678-687, July 2010.

[17] M. Kettler, L. Gerit and H. Unterweger, "Tests on bolted steel angles in compression with varying end support conditions," *Proceedings of the Annual Stability Conference Structural Stability Research Council,* 10-13 April 2018.

[18] M. Vild, V. Chalupa, L. Sabatka and F. Wald, "Advanced analysis of members with gusset plate joints," *Modern Trends in Research on Steel, Aluminium and Composite Structures -Proceedings of the XIV international conference on metal structures,* pp. 378-384, June 2021.

[19] H. Unterweger and R. Ofner, "Traglast von Verbandsstäben aus Hohlprofilen mit quasi-zentrischen Knotenblechanschluss," *Stahlbau 78, Heft 6,* pp. 425-436, June 2009.

[20] ABAQUS , Reference manual, version 6.16, France: Simulia, Dassault Systöms, 2016.